J Appl Electrochem (2009) 39:277–282
DOI 10.1007/s10800-008-9669-1

ORIGINAL PAPER

Temperature dependence of the electrochemical corrosion characteristics of carbon steel in a salty soil

X. H. Nie · X. G. Li · C. W. Du · Y. F. Cheng

Received: 1 April 2008 / Accepted: 19 September 2008 / Published online: 7 October 2008

Abstract The electrochemical corrosion characteristics of carbon steel in a salty soil at different temperatures were studied by measurements and analyses of potentiodynamic polarization curves, linear polarization resistance and electrochemical impedance spectroscopy. The results showed that the mass-transfer of dissolved oxygen plays an essential role in carbon steel corrosion, and the whole corrosion process is mix-controlled by both activation and mass-transfer steps. Passivity can be developed on carbon steel in the soil at low temperatures. With the increase of temperature, the passive current density increases and the passive potential range decreases. When temperature is elevated to a certain value, 50 °C in this system, passivity cannot be maintained and the steel is dominated by an active dissolution status. Anodic Tafel slope decreases continuously with the increase in temperature, which is mainly due to the enhanced electrode reaction rate at an elevated temperature. Simultaneously, cathodic Tafel slope increases with temperature continuously due to the decrease of the solubility of dissolved oxygen in soil. Since the diffusion activation energy is generally much smaller than the reaction activation energy, the effect of temperature on diffusion is far less than that on electrode reaction rate.

Keywords Corrosion · Carbon steel · Salty soil · Electrochemical measurements

X. H. Nie · X. G. Li · C. W. Du
Materials Science and Engineering School, University of Science and Technology Beijing, Beijing 100083, China

Y. F. Cheng (✉)
Department of Mechanical and Manufacturing Engineering, University of Calgary, Calgary, AB, Canada T2N 1N4
e-mail: fcheng@ucalgary.ca

1 Introduction

Carbon steel components have been used widely in the various underground engineering applications, such as oil/gas pipelines, water pipes, etc. Although coatings and cathodic protection (CP) combine to maintain integrity of the facilities, corrosion may occur frequently on carbon steel substrate due to various reasons, such as coating degradation and CP lost.

Corrosion of carbon steel in soils is an electrochemical process, which could be affected by various environmental factors, including type of soil, soil composition, pH, moisture, salt concentration, oxygen content, temperature, microorganisms, etc. [1–4]. Same as the aqueous corrosion, soil corrosion of the steel depends on the water content of soil and aeration [5, 6]. Moreover, it has also been acknowledged [3, 7] that the soil conductivity is critical to the steel corrosion.

With season alternating, soil temperature changes greatly. It was found that, generally, the corrosion rate of buried carbon steel is higher in Summer and Fall, and lower in Winter and Spring in the same location. Because corrosion potential of steel and oxidative–reductive potential (ORP) vary with temperature, CP will be adjusted correspondingly to protect the underground structures. Kim et al. [8] studied the temperature effects on cathode protection of the buried steel pipe, and found that corrosion current density increases with the increasing temperature. The cathodic potential of -0.85 V_{CSE} (copper sulfate electrode) which could protect the steel pipe effectively at ambient temperature or lower, does not provide sufficient protection at elevated temperatures. As a consequence, a more negative potential, such as -1.346 V_{CSE} at 80 °C, should be applied to protect the pipe.

To date, there have been extensive researches [9–11] conducted in aqueous solutions to study the temperature dependence of corrosion of metals, including carbon steels. However, there has been limited work investigating the carbon steel corrosion in soil directly. In North China, the offshore area is distributed with an extensive network of salty soil. The offshore soil is characterized with a high moisture, high salt content, low resistivity, and low oxygen solubility. It is expected that a high corrosion rate will be encountered on buried carbon steel in such a soil.

In this work, electrochemical measurements including polarization curves, linear polarization, and electrochemical impedance spectroscopy (EIS) were used to investigate the corrosion behavior of carbon steel that was buried in the salty soil taken from field at different temperatures. It is expected that a mechanistic understanding will be obtained about the soil corrosion of buried carbon steel and the associated temperature dependence.

2 Experimental procedures

Specimens for electrochemical tests were made of a carbon steel plate with chemical composition (wt.%): C 0.14, Si 0.13, Mn 0.44, P 0.015, S 0.031, and Fe balance. The metallographic observation showed that the microstructure of the steel (without tempering treatment) was primarily ferrite and pearlite, as shown in Fig. 1. Samples were cut into small squares of 1 cm × 1 cm, and then covered with epoxy resin except test surface, with a working area of 1 cm^2. Each sample was successively polished using silicon carbide emery papers from grit 400, 600, 800 to 1,000, then rinsed with deionized water, and degreased with acetone.

The test soil was taken from Dagang, China, a northern offshore city with the typical salty soil. Sampling depth was about one meter, where the steel components were usually buried. The water content of soil was in the range of 19–24%. The chemical composition and soil pH are listed in Table 1. Prior to tests, the naturally dried soil was baked for 6 h at 105 °C, smashed into pieces with an average size of 1 cm in diameter (the smashed pieces of soils are not always the exactly same, but with a similar size), and then soaked in distilled water up to 20% content. The test temperatures were controlled at 20, 30, 40, 50, 60, and 70 °C using a water bath.

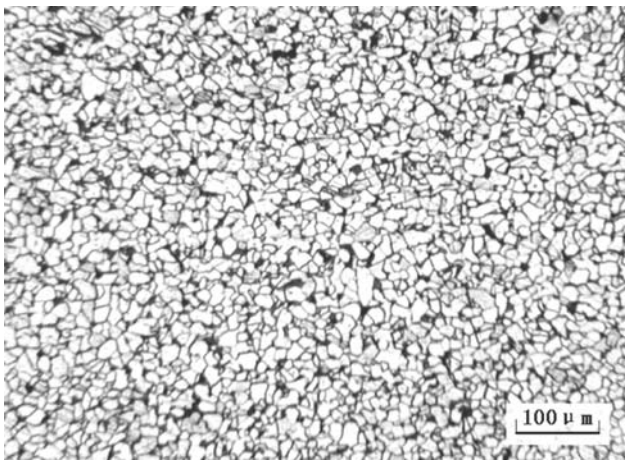

Fig. 1 Metallographic picture showing the microstructure of carbon steel

Table 1 Chemical composition (wt.%) and pH value of the test soil

NO_3^-	Cl^-	SO_4^{2-}	CO_3^{2-}	HCO_3^-	pH
0.01	1.41	0.16	0	0.02	8.8

All the electrochemical measurements were performed on a conventional three-electrode system through a PARSTAT 2273 electrochemical measurement system. Carbon steel specimen was used as working electrode (WE), a saturated calomel electrode (SCE) as reference electrode (RE), and a carbon rod as counter electrode (CE). Prior to electrochemical tests, WE was kept in the test soil for 12 h at the test temperature to ensure that the electrode reached a steady-state, which was indicated by a relatively stable value of corrosion potential of the electrode.

During polarization curve measurements, the potential scanning range was ±500 mV vs. corrosion potential at a scanning rate of 0.333 mV/s. The scanning range for linear polarization measurements was ±10 mV vs. corrosion potential and the scanning rate was 0.167 mV/s. EIS measurements were performed at the open-circuit potential after 12 h of immersion of WE in soil with a frequency range of 200 kHz to 10 mHz and a AC disturbance signal of 10 mV.

3 Results

3.1 Polarization curve measurements

Polarization curves of carbon steel electrode measured at different temperatures in soil are shown in Fig. 2. Electrochemical parameters were fitted from the polarization curves and are listed in Table 2, where E_{corr} is corrosion potential, i_{corr} is corrosion current density, and b_a and b_c are anodic and cathodic Tafel slopes, respectively. It is seen that, with the rising temperature, the anodic current density of steel increased, while there was little change of cathodic current density and corrosion potential. Moreover, the steel could be passivated at low temperatures, such as 20, 30, and 40 °C. When temperature was up to 50 °C, passivity cannot be maintained on steel.

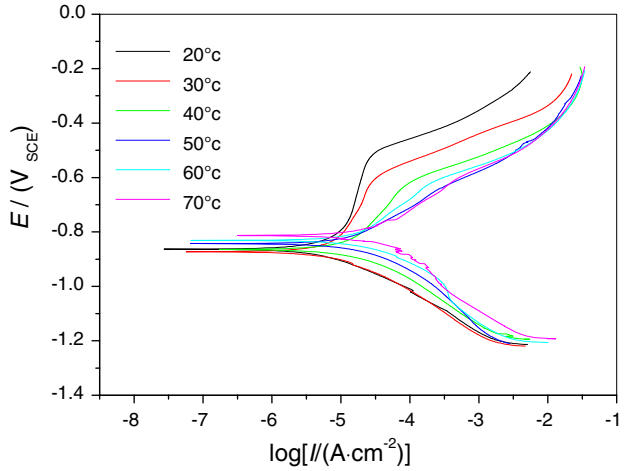

Fig. 2 Polarization curves of carbon steel measured in soil at different temperatures

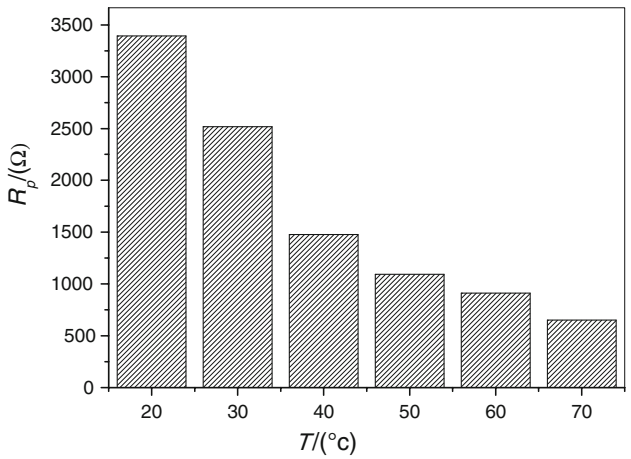

Fig. 3 Linear polarization resistance of carbon steel at different temperatures

Table 2 Electrochemical parameters obtained from polarization curves

T/°C	20	30	40	50	60	70
E_{corr}/mV$_{SCE}$	−722	−711	−695	−707	−706	−694
b_a/(mV dec^{-1})	901	455	290	142	185	164
b_c/(mV dec^{-1})	96	101	116	135	142	202
I_{corr}/(μA cm^{-2})	15.9	16.9	28.2	32.4	54.1	69.2

3.2 Linear polarization measurements

The linear polarization resistances, R_p, measured at different temperatures in soil are shown in Fig. 3. It is seen that R_p decreased continuously with temperature.

3.3 EIS measurements

Nyquist diagrams (a) and Bode plots (b) measured on electrode at different temperatures are shown in Fig. 4. To show more clearly the impedance feature, the EIS plot measured at 20 °C was selected and enlarged in Fig. 5. It is seen that there is a similar feature for EIS diagrams measured at all temperatures, i.e., a depressed semicircle in high frequency range and a Warburg diffusive impedance in low frequency range. Furthermore, the size of the high-frequency semicircle decreased when temperature was increased. The magnitude of impedance decreased with the rising temperature, as shown in Fig. 4b.

The electrochemical equivalent circuit shown in Fig. 6 was used for fitting impedance data, where R_s is solution resistance, R_t is charge-transfer resistance, and CPE is constant phase element. The impedance of CPE is given as:

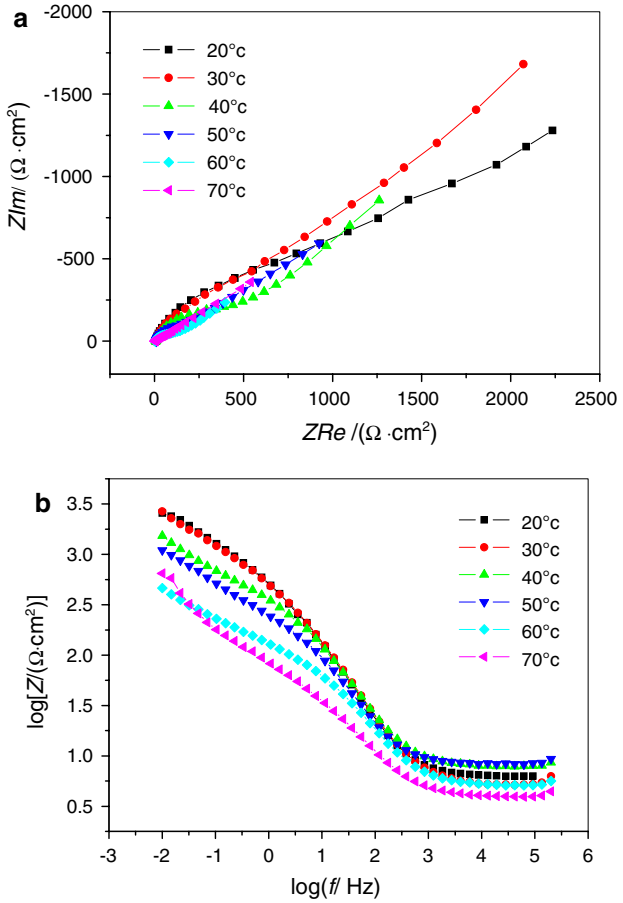

Fig. 4 Nyquist diagrams (**a**) and Bode plots (**b**) of carbon steel measured in soil at different temperatures

$$Z_{CPE} = \frac{1}{Y_0(j\omega)^n} \quad (1)$$

where Y_0 is the magnitude of CPE, and $-1 \leq n \leq 1$. Warburg impedance, Z_W, in Fig. 6 is used to describe the

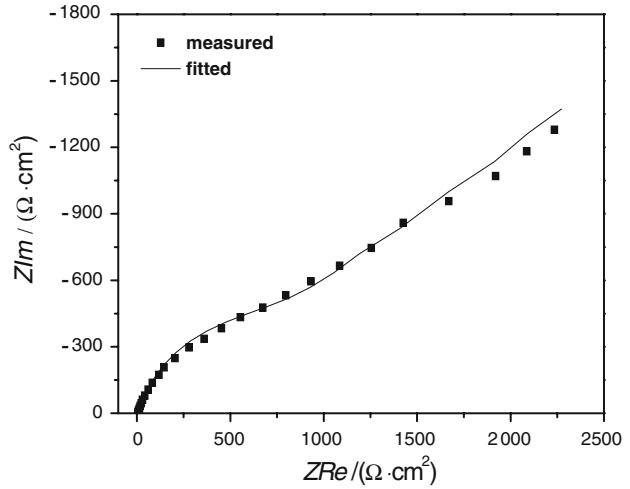

Fig. 5 EIS plot measured at 20 °C and the fitted curve

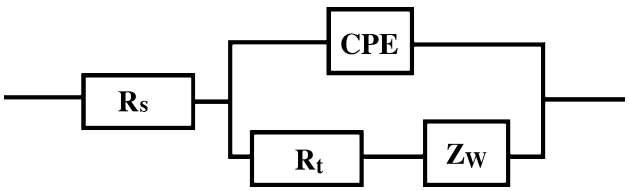

Fig. 6 Electrochemical equivalent circuit to fit the impedance data

diffusive characteristic of reactant or resultant. The impedance of Z_W is expressed as:

$$Z_W = \frac{1}{Y_{0W}}(j\omega)^{-\frac{1}{2}} = \frac{\sigma}{\sqrt{\omega}} - j\frac{\sigma}{\sqrt{\omega}} \quad (2)$$

where σ is Warburg coefficient, and Y_{0W} is admittance. It is seen from Fig. 5 that the experimental data and the fitted curve fit very well. The results of the fitted parameters are shown in Table 3, and the temperature dependence of charge-transfer resistance is shown in Fig. 7. It is clear that R_t decreased with the increasing temperature.

4 Discussion

4.1 Electrochemical corrosion characteristics of carbon steel in salty soil and the temperature dependence

Generally, the anodic and cathodic reactions of carbon steel corrosion in aerated, neutral or alkaline solution are expressed as follows:

$$Fe \rightarrow Fe^{2+} + 2e^- \quad (3)$$

$$O_2 + 2H_2O + 4e^- \rightarrow 4OH^- \quad (4)$$

Oxygen dissolves and diffuses through the soaked soil towards the steel electrode surface for reduction reaction. The presence of low-frequency diffusive impedance in EIS

Table 3 Electrochemical parameters fitted from the impedance data at different temperatures

T/°C	R_s/Ω	Y_{0w}/(S·s^n)	n	R_t/Ω	Y_{0w}/(S·s$^{0.5}$)
20	6.2	2.70E−04	0.803	862	1.70E−03
30	5.3	2.40E−04	0.805	604	1.40E−03
40	7.9	2.80E−04	0.792	402	3.20E−03
50	8.4	3.20E−04	0.805	232	3.60E−03
60	5.1	5.90E−04	0.725	127	1.00E−02
70	4	9.90E−04	0.729	59	6.90E−03

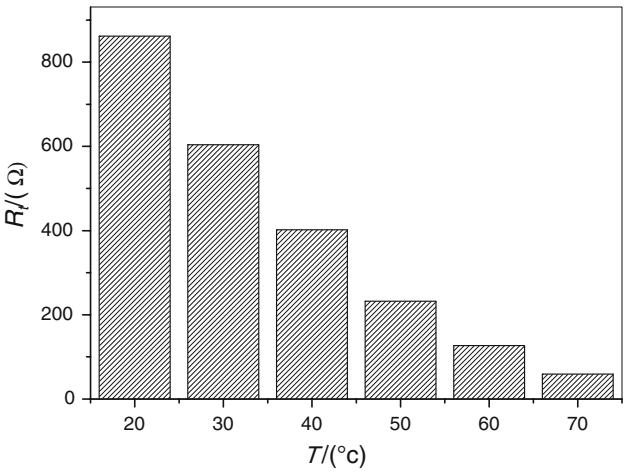

Fig. 7 Charge-transfer resistance of carbon steel in soil at different temperatures

plots (Fig. 4a) suggests that mass-transfer of dissolved oxygen plays an essential role in carbon steel corrosion, and the whole corrosion process is mixed-controlled by activation and diffusion steps. Furthermore, a comparison of linear polarization resistance, R_p (Fig. 3), and charge-transfer resistance, R_t (Table 3) measured at different temperatures shows that the former is always larger than the latter at individual temperature. As a DC measurement technique, R_p represents the resistance of whole electrode reaction [12]. However, R_t determined from EIS measurement represents the resistance for charge-transfer step only. When the electrode process is dominated by activation step and the effect of mass-transfer step is negligible, R_p is equal to R_t. Apparently, in the present electrode reaction process, mass-transfer step plays a significant role, and corrosion of carbon steel in present soil system is co-controlled by both activation and mass-transfer steps.

Passivity of carbon steel at low temperature is mainly due to formation of iron oxides in soaked soil by:

$$Fe + H_2O + OH^- \rightarrow Fe(OH)_2 + H^+ + 2e \quad (5)$$

$$4Fe(OH)_2 + O_2 \rightarrow 2Fe_2O_3 + 4H_2O \quad (6)$$

With increase of temperature, the solubility of oxygen in soaked soil decreases [13] although the oxygen diffusivity

increases. Furthermore, the dissolution activity of steel increases with temperature. Therefore, passive current density increases and passive potential range decreases with the increase in temperature. When temperature is elevated to a certain value, 50 °C in this system, passivity cannot be maintained and the steel is dominated by active dissolution status.

4.2 Effect of temperature on electrochemical reaction parameters

Anodic Tafel slope, b_a, decreases continuously with the increase in temperature, as seen in Table 2. It is mainly due to the enhanced electrode reaction rate at an elevated temperature. An empirical relationship between b_a and temperature obtained in this work can be described by:

$$b_a = 144.2 + 4,593.5 \exp\left(-\frac{T}{11.1}\right) \quad (7)$$

The cathodic Tafel slope, b_c, increases with temperature continuously (Table 2). It is attributed to the decrease of solubility of dissolved oxygen in soil with the rising temperature. As a consequence, cathodic reduction reaction of oxygen on electrode surface is inhibited, resulting in a high cathodic Tafel slope at the elevated temperature.

Linear polarization measurement is usually used to determine corrosion rate. Corrosion current density can be calculated through R_p by Stern equation:

$$I_{corr} = \frac{B}{R_p} \quad (8)$$

where B is a constant and can be obtained from cathodic/anodic Tafel slopes by

$$B = \frac{b_a b_c}{2.303(b_a + b_c)} \quad (9)$$

The calculated values of B at different temperature are listed in Table 4. The calculated values of B in Table 4 vary from 30.1 to 39.3 mV, with a mean value of 35.6 mV.

Furthermore, the relationship between I_{corr} and $1/R_p$ is plotted in Fig. 8, and a straight line can be fitted from the experimental data, with a slope of 44.2 mV. It is apparent that the fitted value of Stern constant B is very close to that calculated from the Tafel slopes. The value of 44.2 mV could be used to calculated corrosion rate of carbon steel in the salty soil.

Table 4 Linear polarization resistance and the value of B at different temperatures

T/°C	20	30	40	50	60	70
R_p/(Ω cm^2)	3,394	2,519	1,476	1,093	911	651
B/mV	37.7	35.9	36.0	30.1	34.9	39.3

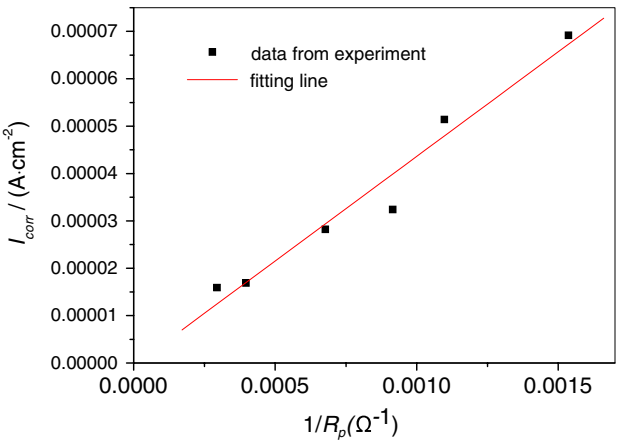

Fig. 8 Relationship between corrosion current density and $1/R_p$

4.3 Effect of temperature on corrosion rate of carbon steel

The present work shows that an increase in temperature within the test range accelerates corrosion of carbon steel in the salty soil. The relationship between reaction rate constant, k, and temperature is by Arrhenius formula:

$$\ln k = -\frac{E_R}{RT} + B \quad (10)$$

where R is ideal gas constant, and E_R is reaction activation energy (J/mol). Apparently, reaction rate constant and thus the corrosion rate increase when temperature increases.

Furthermore, the oxygen solubility in soil or solution decreases with temperature. Despite the increase of the oxygen diffusivity, the temperature dependence of diffusion coefficient, D, can be expressed by:

$$D = D_0 e^{-\frac{E_D}{RT}} \quad (11)$$

where E_D is diffusion activation energy. In general, E_D is much smaller than reaction activation energy, E_R. Therefore, the effect of temperature on diffusion is far less than that on electrode reaction rate. Generally, according to the values of activation energy, the electrode reaction rate will increase 10–100 times if diffusion rate is doubled.

For corrosion reaction with the oxygen reduction as cathodic process, generally, the corrosion rate of steel reaches the maximum at about 80–90 °C. When temperature increases further, corrosion rate decreases. It is attributed to the significant reduction in oxygen content in aqueous solution or soaked soil, and simultaneously, the formation of a more compact oxide film on electrode surface at the elevated temperature [13].

5 Conclusions

(i) Mass-transfer of dissolved oxygen plays an essential role in carbon steel corrosion, and the whole corrosion process is mix-controlled by both activation and mass-transfer steps.

(ii) Passivity can be developed on carbon steel in soil at low temperatures. With the increase of temperature, the passive current density increases and the passive potential range decreases. When temperature is elevated to a certain value, 50 °C in this system, passivity cannot be maintained and the steel is dominated by active dissolution status.

(iii) Anodic Tafel slope decreases continuously with the increase in temperature, which is mainly due to the enhanced electrode reaction rate at an elevated temperature. Simultaneously, cathodic Tafel slope increases with temperature continuously due to the decrease of solubility of dissolved oxygen in soil.

(iv) Since diffusion activation energy is generally much smaller than reaction activation energy. Therefore, the effect of temperature on diffusion is far less than that on electrode reaction rate. The corrosion rate of steel increases when temperature is risen.

Acknowledgments This work was supported by National Science and Technology Planning Project of China (2006BAK02B01-06), Chinese National R and D Infrastructure and Facility Development Program (2005DKA10400), and Canada Research Chair Program.

References

1. Hoffmeister H (2005) Corrosion 61:880
2. Gerwin W, Baumhauer R (2000) Geoderma 96:63
3. Osella A, Favetto A (2000) J Appl Geophys 44:303
4. Ferreira CAM, Ponciano JAC, Vaiteman DS (2007) Environment 388:250
5. Gardiner CP, Melchers RE (2002) Corros Sci 44:2459
6. Levlin E (1996) Corros Sci 38:2083
7. Li SY, Jung S, Park K (2007) Mater Sci Commun 103:9
8. Kim JG, Kim YW (2001) Corros Sci 44:2011
9. Li DG, Feng YR, Bai ZQ (2007) Electrochimica Acta 52:7877
10. Takasaki S, Yamada Y (2007) Corros Sci 49:240
11. Popova A (2007) Corros Sci 49:2144
12. Kouřil M, Novák P, Boiko M (2006) Cem Concr Comp 28:220
13. Cheng YF, Steward FR (2004) Corros Sci 46:2405